Development of a Photogrammetric Processing Workflow for UAV-based Multispectral Imagery

Student Research Colloquium 2017
Forest **I**nformation **T**echnology (M.Sc.)
4th Semester
Max Kampen

Universität für Bodenkultur Wien
Department für Raum, Landschaft
und Infrastruktur

HNE Eberswalde
Eberswalde University for Sustainable Development
University of Applied Sciences

General Information

3rd Semester's Research project was part of a feasibility study carried out by the Institute of Surveying, Remote Sensing and Land Information (IVFL) at the University of Natural Resources and Life Sciences, Vienna

Universität für Bodenkultur Wien
Department für Raum, Landschaft und Infrastruktur

Content

- Introduction
- Methodology
- Results
- Conclusions

Supervisor

Dipl.-Ing. Markus Immitzer MSc.

Peter-Jordan-Straße 82

1190 Wien

Email: markus.immitzer(at)boku.ac.at

Tel: +43 1 47654-85732

Introduction

- Flexibility is of crucial importance when monitoring forest disturbances like bark beetle (*Ips typographus* or *Pityogenes chalcographus*) infestation in order to develop mitigation strategies and initiate timely countermeasures
- **Satellite remote sensing** is too inflexible and **terrestrial monitoring** too time-consuming and cost-intensive

Introduction

- Research group aims to develop a data acquisition and processing method for multitemporal UAV-based multispectral imagery, which could enable flexible low-cost monitoring of tree species distribution and forest disturbances

Objectives & Research Questions

- Development of a photogrammetric processing workflow
- Is it possible to sufficiently distinguish different tree species by their spectral signatures?
- Is it possible to detect differences in health statuses between individual trees?

Literature Research

Early Detection of Bark Beetle Infestation in Norway Spruce (*Picea abies*, L.) using WorldView-2 Data

MARKUS IMMITZER & CLEMENT ATZBERGER, Vienna, Austria

Keywords: WorldView-2, bark beetle infestation, tree vitality, green-attack, pre-visual detection, Norway spruce

Taylor & Francis

...OF A MULTISPECTRAL UAV PHOTOGRAMMETRY FOR DETECTION AND TRACKING OF FOREST DISTURBANCE DYNAMICS

R. Minařík [a], J. Langhammer [a,*]

...ysical Geography and Geoecology, Faculty of Science, Charles University in Prague, ... Czech Republic - (robert.minarik, jakub.langhammer)@natu...

Forestry applications of UAVs in Europe: a re...

Chiara Torresan ...

Forecasting potential bark beetle outbreaks based on spruce forest vitality using hyperspectral remote-sensing techniques at different scales

A. Lausch [a,*], M. Heurich [b], D. Gordalla [c], H.-J. Dobner [c], S. Gwillym-Margianto [d], C. Salba...

[a] UFZ, Helmholtz Centre for Environmental Research - UFZ, Department of Computational Landscape Ecology, Permoserstraße 15, D-04318 Leipzig, G...
[b] Bavarian Forest National Park, D-94481 Grafenau, Germany
[c] Leipzig University of Applied Science – HTWK Leipzig, Karl-Liebknecht-Straße 132, D-04277 Leipzig, Germany
[d] UFZ, Helmholtz Centre for Environmental Research - UFZ, Department of Community Ecology, Theodor-Lieser-Straße 4, D-06120 Halle, Germany

MDPI

remote sensing

Article

Individual Tree Detection and Classification with UAV-Based Photogrammetric Point Clouds and Hyperspectral Imaging

Olli Nevalainen [1,*], Eija Honkavaara [1], Sakari Tuominen [2], Niko Viljanen [1], Teemu Hakala [1], Xiaowei Yu [1], Juha Hyyppä [1], Heikki Saari [3], Ilkka Pölönen [4], Nilton N. Imai [5] and Antonio M. G. Tommaselli [5]

ISSN 2072-4292
www.mdpi.com/journal/remotesensing

Article

Using UAV-Based Photogrammetry and Hyperspectral Imaging for Mapping Bark Beetle Damage at Tree-Level

Roope Näsi [1], Eija Honkavaara [1,*], Päivi Lyytikäinen-Saarenmaa [2], Minna Blomqvist [2], Paula Litkey [1], Teemu Hakala [1], Niko Viljanen [1], Tuula Kantola [2], Topi Tanhuanpää [2] and Markus Holopainen [2]

OPEN ACCESS

forests

ISSN 1999-4907
www.mdpi.com/journal/forests

Article

Analysis of Unmanned Aerial System-Based CIR Images in Forestry—A New Perspective to Monitor Pest Infestation Levels

Jan Rudolf Karl Lehmann [1,*], Felix Nieberding [1], Torsten Prinz [2] and Christian Knoth [2]

Literature Research

	A	B	C	D	E	F	G	H	I
1	Author&Title	Subject	Goals	Species	Material	Methods	Data Processing & Image analysis	Output	Notes
6	Fassnacht, F. E., Latifi, H., Ghosh, A., Joshi, P. K., & Koch, B. (2014) Assessing the potential of hyperspectral imagery to map bark beetle-induced tree mortality	tree detection and classification detection of bark beetle infestation	- assess mapping accuracies of bark beetle-induced tree mortality in 3 scenarios with differing target classes - identify crucial spectral regions to map bark beetle-induced tree mortality	Mainly Norway spruce - Picea abies Bark beetle - Ips typographus	- HyMap hyperspectral data (airplane) - Airborne CIR imagery	- corrections in ATCOR4 and ORTHO software - HyMap and CIR images co-registered - CIR-based training samples for tree mortality classes as reference data -> Green Mortality Stage,Early Mortality Stage, Late Mortality Stage, Healthy Coniferous, Healthy Broadleaved, Bare Soil, Sparsely vegetated	- samples for tree mortality classes selected with manually drawn polygons in CIR images - Genetic Algorithm (GA) for hyperdimensional classification - parameter tuning for classification - SVM classifier used	- reported accuracies for delineation of early mortality stages were rather low, so that a combination of genetic algorithm and supervised classification was not sufficient for feature separation - substantial over- classification of the Green Mortality Stage class, which in turn can be explained by the double confusion with the Healthy Coniferous and the Early Mortality Stage class - main problem associated with accurate mapping of late mortality stages is rather differentiating among dead trees, bare soil and sparsely vegetated soil (possible to improve with height information) - Genetic algorithm selected green peak (approx. 560 nm), the chlorophyll absorption feature (680 nm) and the red-edge (690 nm) as bands contributing most to high classification accuracies	- NIR plateau (1076 nm, 1069 nm) and 1532 nm have been found to be good estimators of water content and vegetation damage
7	Lausch, A., Heurich, M., Gordalla, D., Dobner, H. J., Gwillym-Margianto, S., & Salbach, C. (2013) Forecasting potential bark beetle outbreaks based on spruce forest vitality using hyperspectral remote-sensing techniques at different scales.	detection of bark beetle infestation	prediction of outbreak potential of bark beetle infestation based on detection of different vitality stages of spruce that provide prediction indicators	Norway spruce - Picea abies Bark beetle - Ips typographus	- HyMap hyperspectral data (airplane)	- classification of 5 different spruce vitality conditions/infestation stages from different years using long time vector data and hyperspectral data (resolutions 4m & 7m) - ID3 decision tree classification method	- pixel-based 4m & 7m - ATCOR4 & ORTHO - ENVI 4.7	- Important spectral information for derivation vitality status of spruce are 450–890 nm - Hyperspectral data with 4 m grain contain more relevant information to estimate differences in vitality of spruce than 7 m - limited use of spectral information 1400-1800 nm (part of SWIR) - insufficient differentiation accuracy between early stage and healthy class	450-890 nm: wavebands related to prominent chlorophyll absorption features 1400-1800 nm: reflects the water content of needles
8	Yuan, Y., & Hu, X. (2016) Random forest and objected-based classification for forest pest extraction from uav aerial imagery	detection of forest pests	presenting random forest and object-based classification for forest pest detection in UAV aerial imagery		- UAV imagery	- segmentation of image into "superpixels" - The zero parameter version of the SLIC algorithm is used for choosing an adaptive compactness factor - random forest (algorithm) model and validated classification	- image segmentation is performed by the simple lineariterative clustering (SLIC) algorithm proposed by R. Achanta in2012(R. Achanta et al., 2012)	- approach can effectively detect all of the visually salient pest areas from the UAV imagery - high potential of UAV aerial imagery for forest pest infestation monitoring - strong positive economic advantage over the traditionally applied ground based forest pest detection - limited data amount, algorithm needs to be tested for different conditions	"random forest is much faster in training and testing than traditional classifiers (such as an SVM)" said to be robust to outlying observations

Fig. 1: Screenshot of information table created during literature research

UAV - Setup

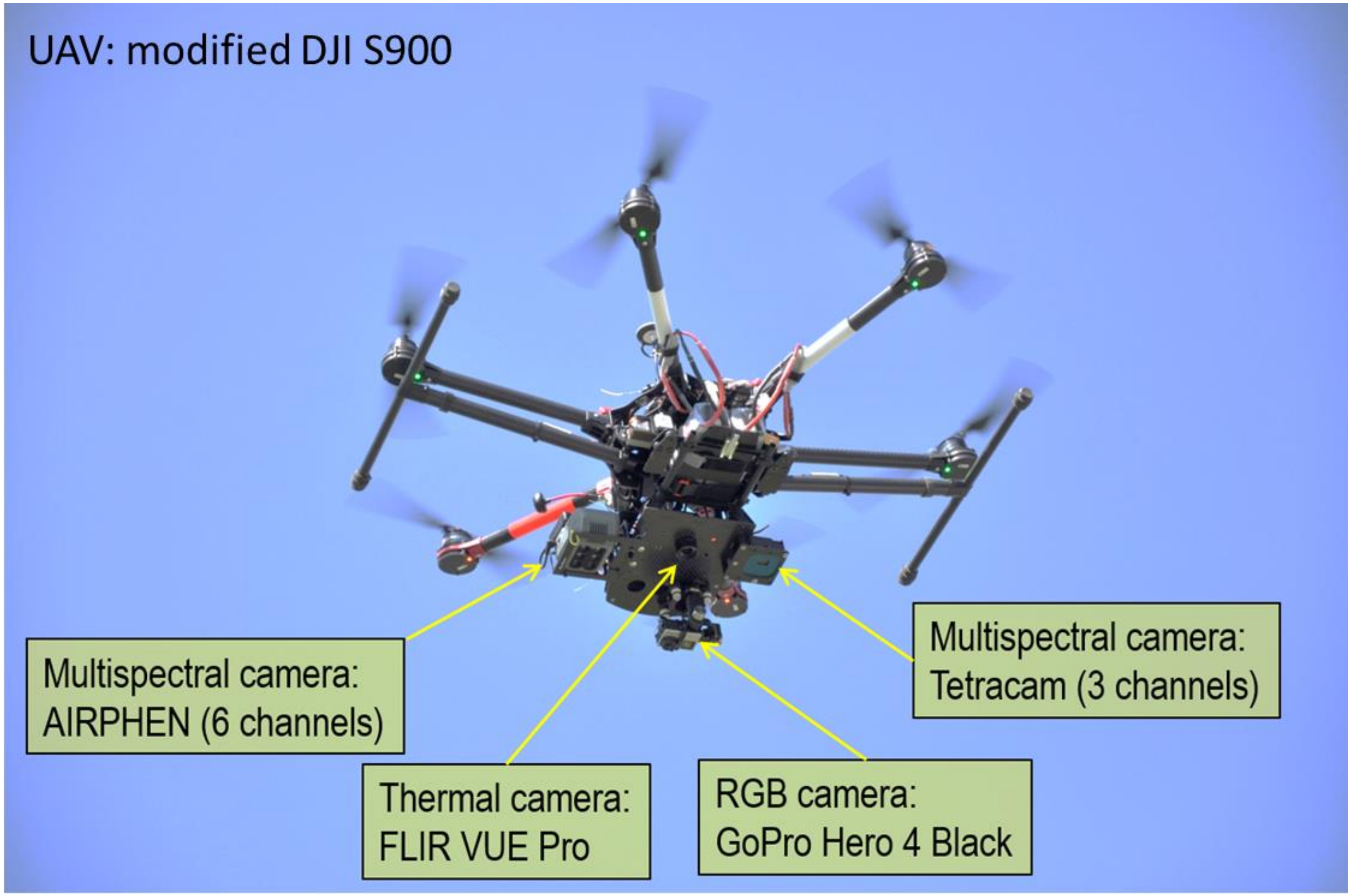

Fig. 2: UAV-Setup with all four jointly mounted camera systems. (Arrows indicate position of the respective camera)

Camera Systems

Table 1: Specifications of utilized cameras

Camera system	Imagery	Wavelengths	Resolution [pixels]
GoPro Hero 4 Black	3-band-RGB	400 – 700 nm	4000 x 3000
Tetracam ADC Snap	3-band-multispectral	520 – 920 nm	1280 x 1024
AIRPHEN	6-band-multispectral	450 – 850 nm	1280 x 960
FLIR VUE Pro Thermal	1-band-thermal	7.5 – 13.5 µm	640 x 512

Fig. 3: Tetracam ADC Snap

Fig. 4: AIRPHEN

Camera Systems

Table 1: Specifications of utilized cameras

Camera system	Imagery	Wavelengths	Resolution [pixels]
GoPro Hero 4 Black	3-band-RGB	400 – 700 nm	4000 x 3000
Tetracam ADC Snap	3-band-multispectral	520 – 920 nm	1280 x 1024
AIRPHEN	6-band-multispectral	450 – 850 nm	1280 x 960
FLIR VUE Pro Thermal	1-band-thermal	7.5 – 13.5 µm	640 x 512

Fig. 5: CIR-image recorded by Tetracam ADC Snap

Fig. 6: Image recorded by AIRPHEN 450nm band

Camera Systems

Table 1: Specifications of utilized cameras

Camera system	Imagery	Wavelengths	Resolution [pixels]
GoPro Hero 4 Black	3-band-RGB	400 – 700 nm	4000 x 3000
Tetracam ADC Snap	3-band-multispectral	520 – 920 nm	1280 x 1024
AIRPHEN	6-band-multispectral	450 – 850 nm	1280 x 960
FLIR VUE Pro Thermal	1-band-thermal	7.5 – 13.5 µm	640 x 512

Fig. 5: CIR-image recorded by Tetracam ADC Snap

Fig. 6: Image recorded by AIRPHEN 450nm band

! Focus on most promising system !

Investigation Area

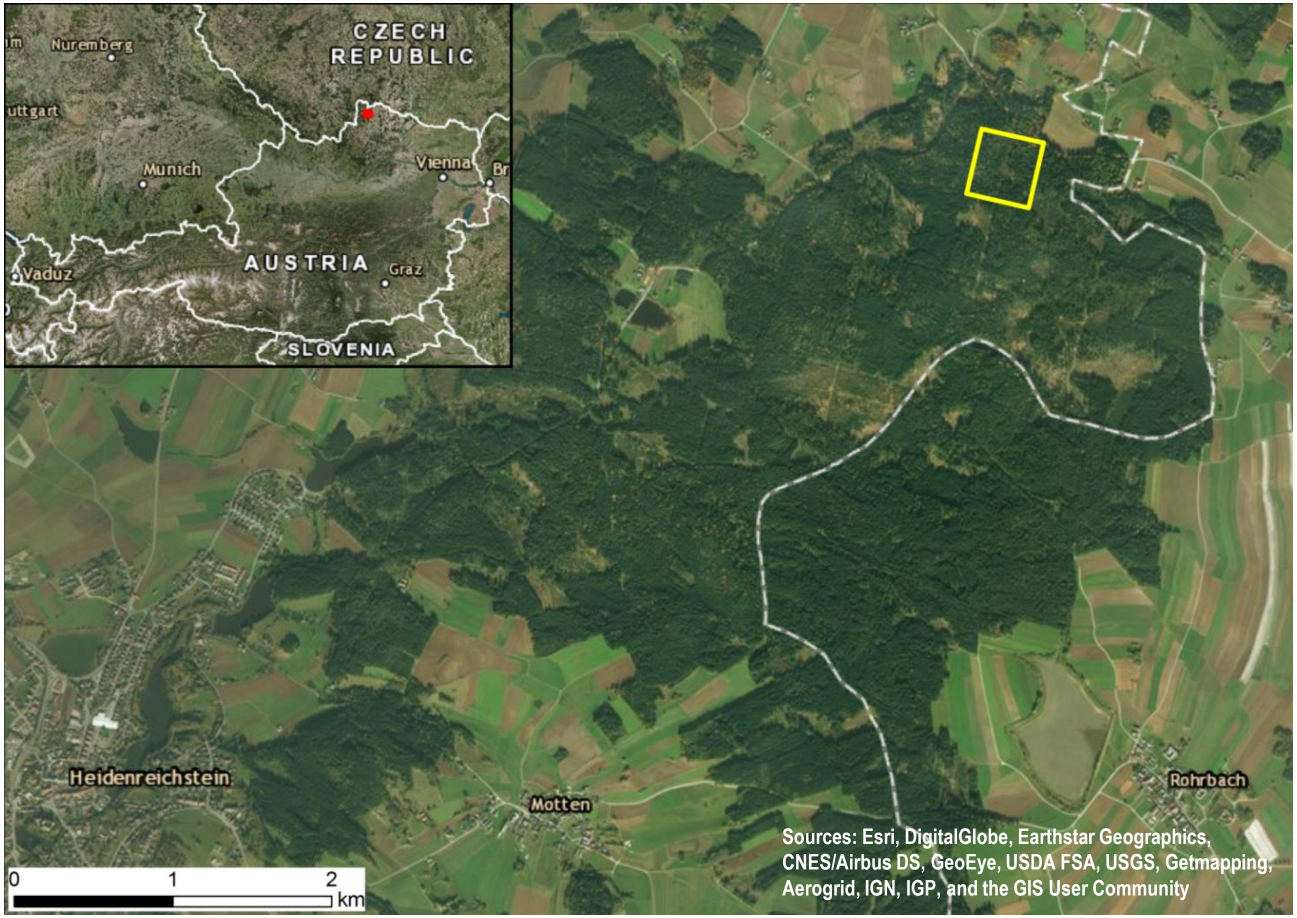

Fig. 7: Location map of the investigation area showing the position within Austria (red mark) in the upper left corner and the approximate position and extent of the study site (yellow mark) close to Heidenreichstein.

Data Acquisition

- 10 flight survey days (May – September 2016)
- Adjusted flight altitude and speed to cover investigation area with one battery charge
- Inhomogeneous data due to different weather conditions and luminosity changes during flights
- Tetracam recorded 300 images/flight
- AIRPHEN recorded around 650 images/flight for all 6 spectral bands (450, 530, 560, 675, 730 and 850 nm)

Processing

- Creation of camera calibration files with ***Agisoft Lens 0.4.2*** to account for each camera's inner orientation
- Photogrammetric processing (point clouds, 3D-models, DEMs and orthomosaics) performed in ***Agisoft PhotoScan professional 1.2.6***
- Creation of tree crown mask for object-based analysis in ***ArcGIS 10.3***
- Layer stacking and analysis of crown pixel values (DN) performed with ***raster*** package (Hijmans & van Etten, 2014) in ***RStudio***

General Workflow

1. Image Matching → Sparse Point Cloud
2. Optimizing Image Orientation → Marking GCPs
3. Dense Point Cloud Computing & Editing
4. Creation of 3D-Model & Texture
5. Creation of Digital Surface Model (DSM)
6. Compute Orthomosaic

!!!! Processing parameters were adjusted according to initial processing trials and evaluation !!!!

1. Image Matching

Table 2: Parameter settings for the image alignment and sparse cloud generation in Agisoft PhotoScan

Parameters	Settings	
Accuracy	Medium	High
Pair selection	Generic	Generic
Key point limit	40,000	40,000
Tie point limit	2,000	4,000
Adaptive camera model fitting	Enabled	Enabled

1. Image Matching

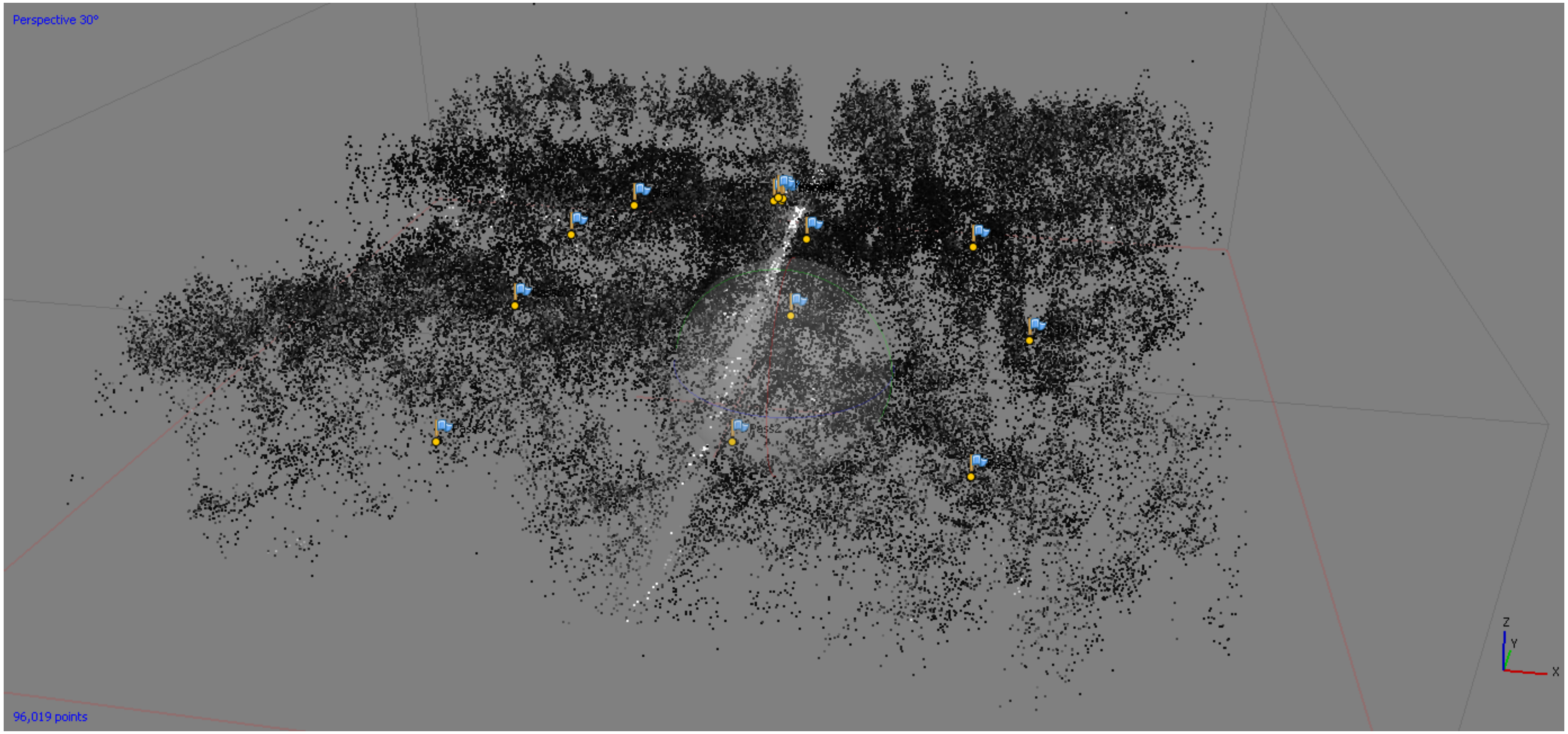

Fig. 8: Sparse Cloud derived from AIRPHEN 450nm band imagery through image matching / alignment process

2. Optimizing Image Orientation

Fig. 9: Image from AIRPHEN 450nm band with a marked ground control point (GCP)

Difficulties Marking GCPs

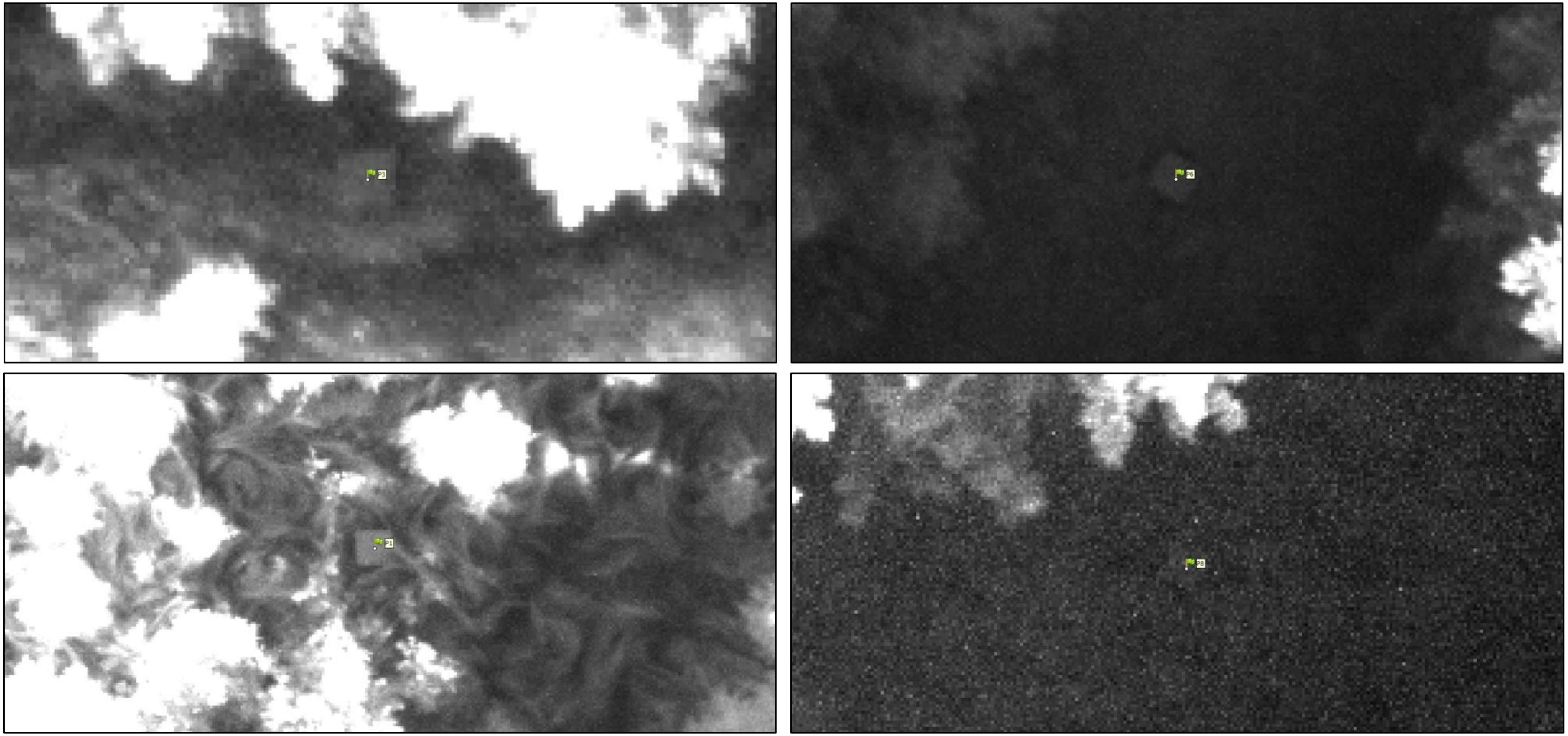

Fig. 10: Images of AIRPHEN imagery depicting difficult conditions for marking of GCPs

3. Dense Point Cloud Computing & Editing

- Dense cloud quality and depth filtering proved to be most influential parameters for tree representation in later orthomosaics

- Quality: Ultrahigh
- Depth filtering: Mild

3. Dense Point Cloud Computing & Editing

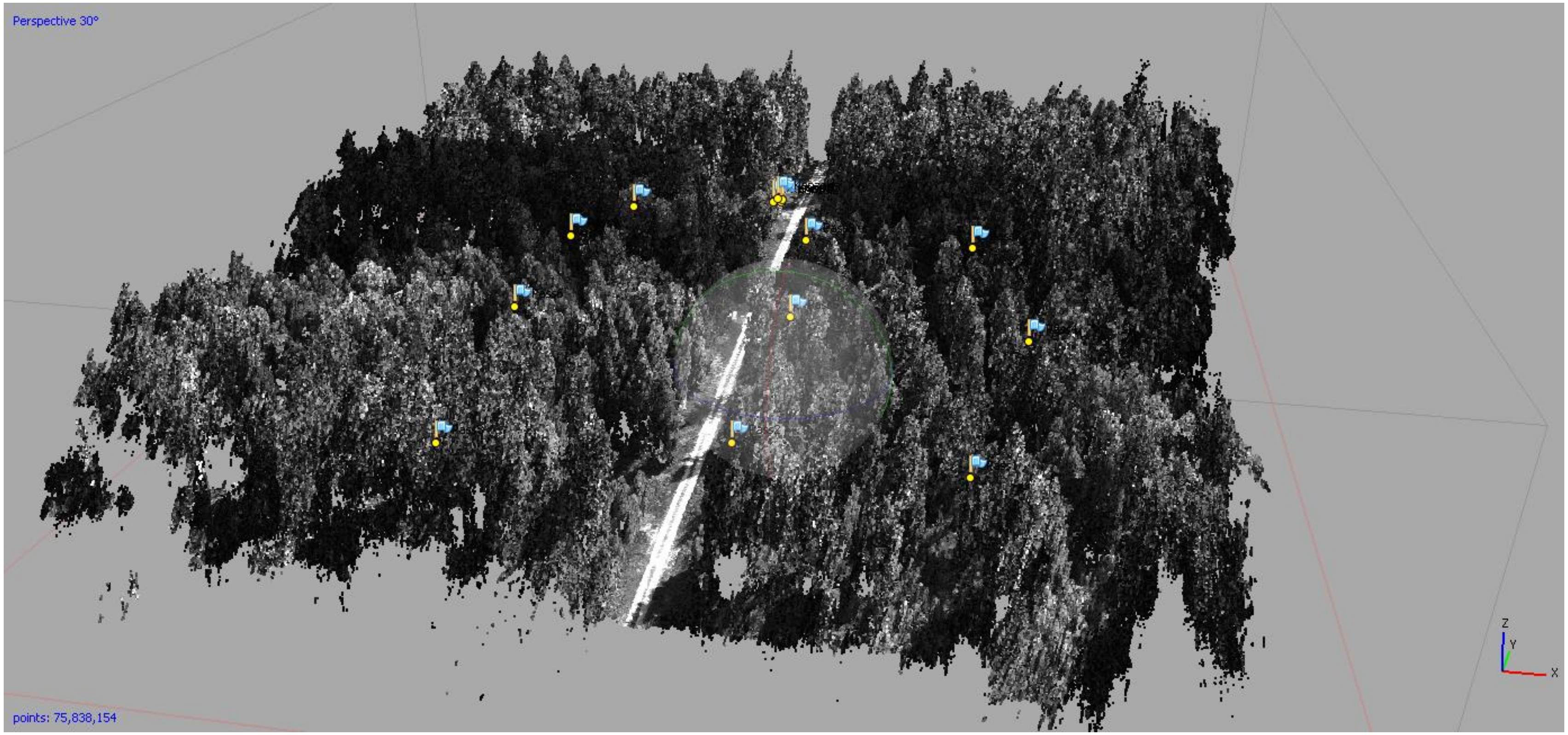

Fig. 11: Sparse Cloud derived from AIRPHEN 450nm band imagery through image matching / alignment process

3. Dense Point Cloud Computing & Editing

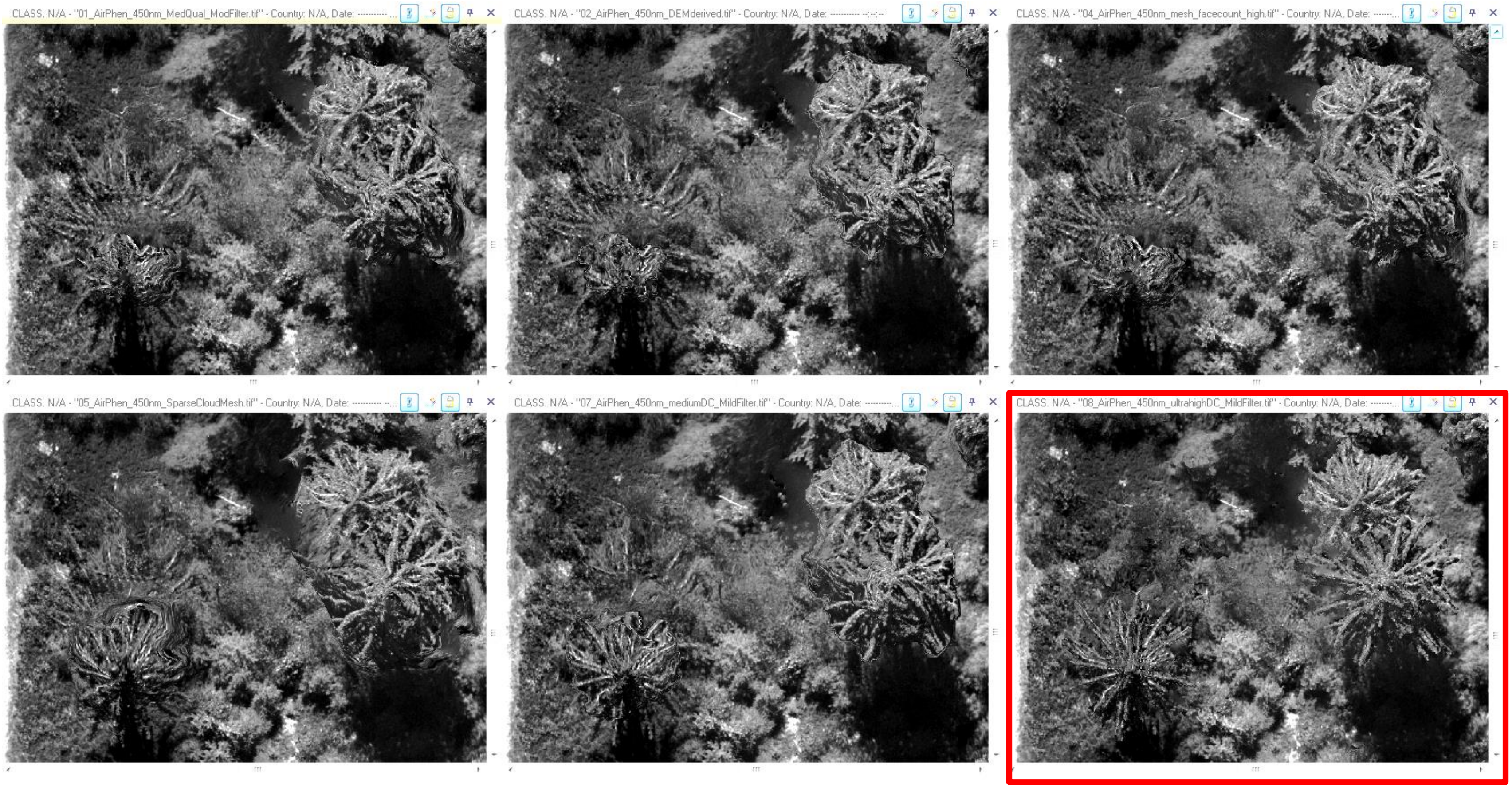

Fig. 12: Comparison of tree features in differently processed orthomosaics from AIRPHEN 450nm band imagery (red frame indicating optimal quality and depth filtering settings for dense point clouds)

3. Dense Point Cloud Computing & Editing

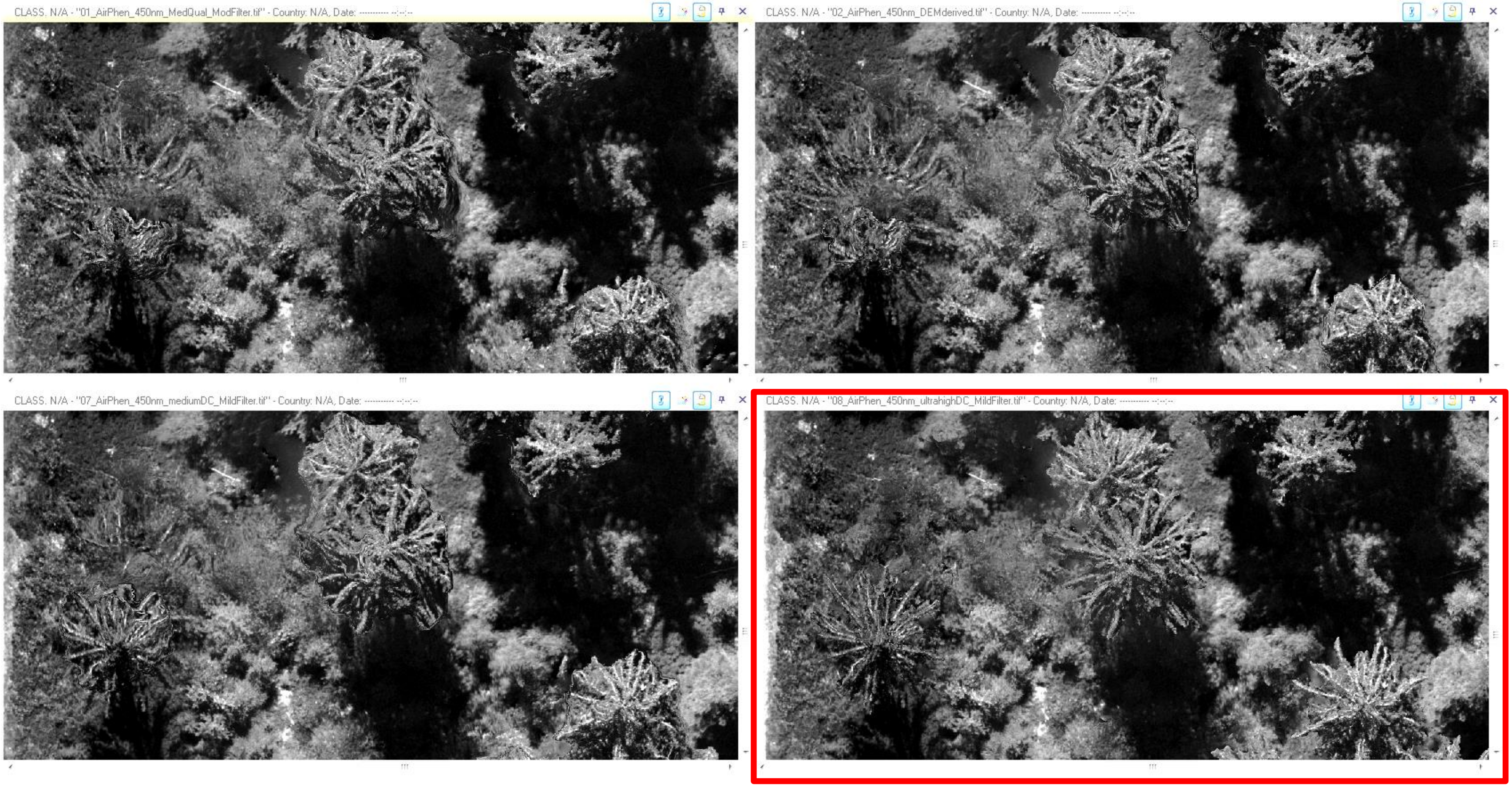

Fig. 13: Comparison of tree features in differently processed orthomosaics from AIRPHEN 450nm band imagery (red frame indicating optimal quality and depth filtering settings for dense point clouds)

3. Dense Point Cloud Computing & Editing

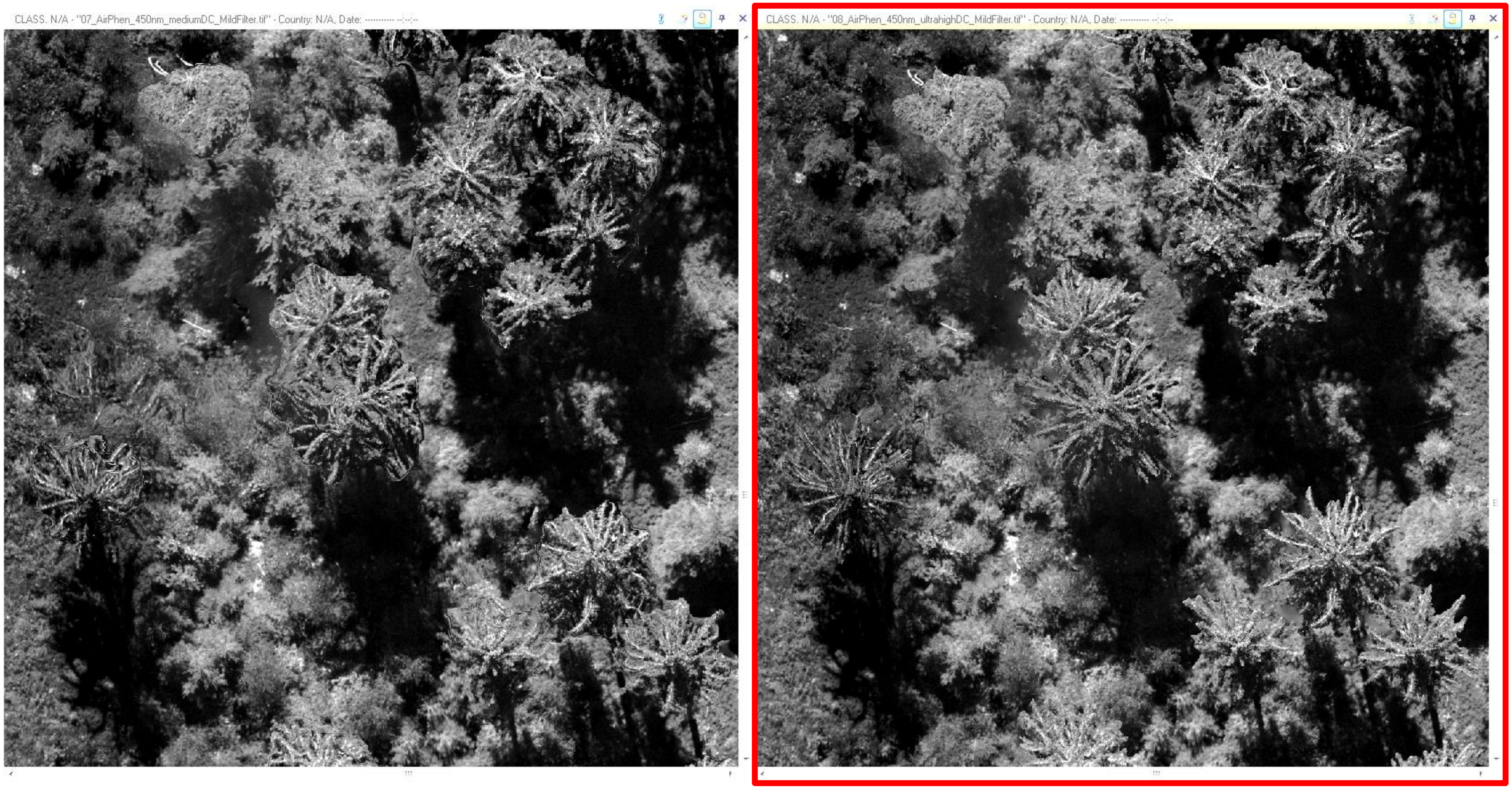

Fig. 14: Comparison of tree features in differently processed orthomosaics from AIRPHEN 450nm band imagery (red frame indicating optimal quality and depth filtering settings for dense point clouds)

3. Dense Point Cloud Computing & Editing

- Manual removal of outliers above canopy height and under ground level (necessary for correct DSM)

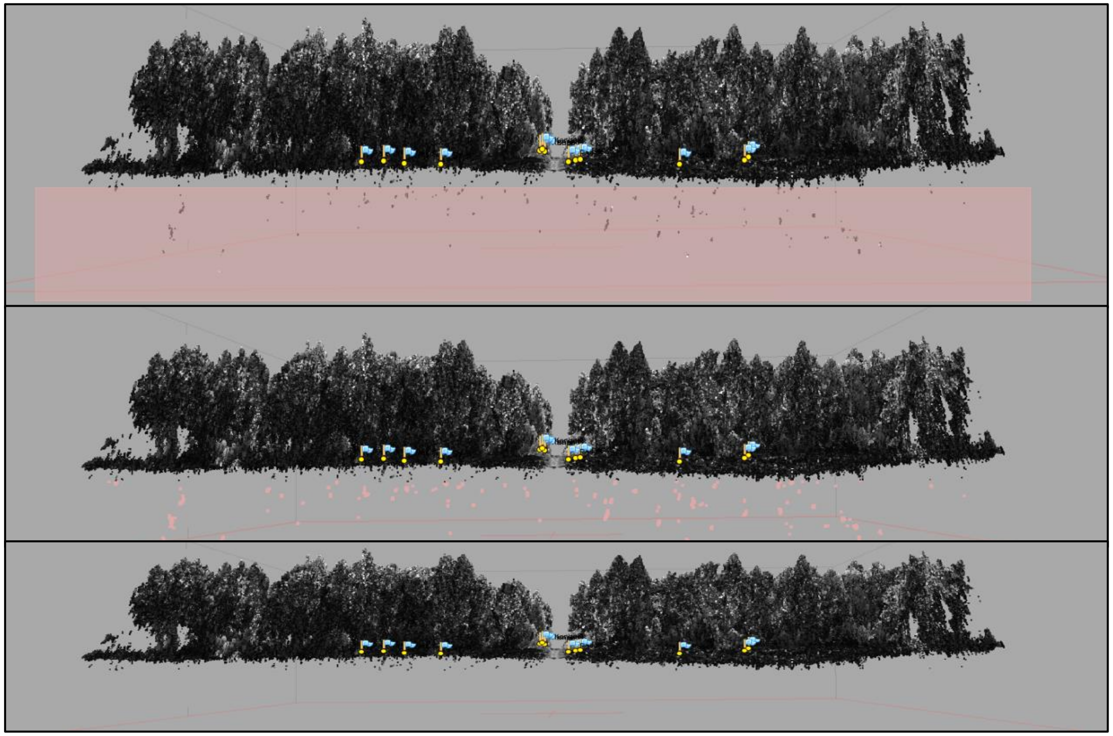

Fig. 15: Screenshots depicting manual removal of outliers in a dense cloud derived from AIRPHEN imagery

4. Creation of 3D-Model & Texture

- Just intermediate steps
- Highlighted settings were recommended for aerial imagery

Table 3: Settings for 3D-Model creation

Parameters	Settings
Surface type	Height field
Blending mode	Mosaic (default)
Face count	Medium (default)
Interpolation	Enabled

Table 4: Settings for Texture creation

Parameters	Settings
Mapping mode	Orthophoto
Blending mode	Mosaic (default)
Texture size/count	4096 (default)
Color correction	Disabled
Hole filling	Enabled

5. Creation of Digital Surface Model (DSM)

- DSM was derived from the dense point cloud

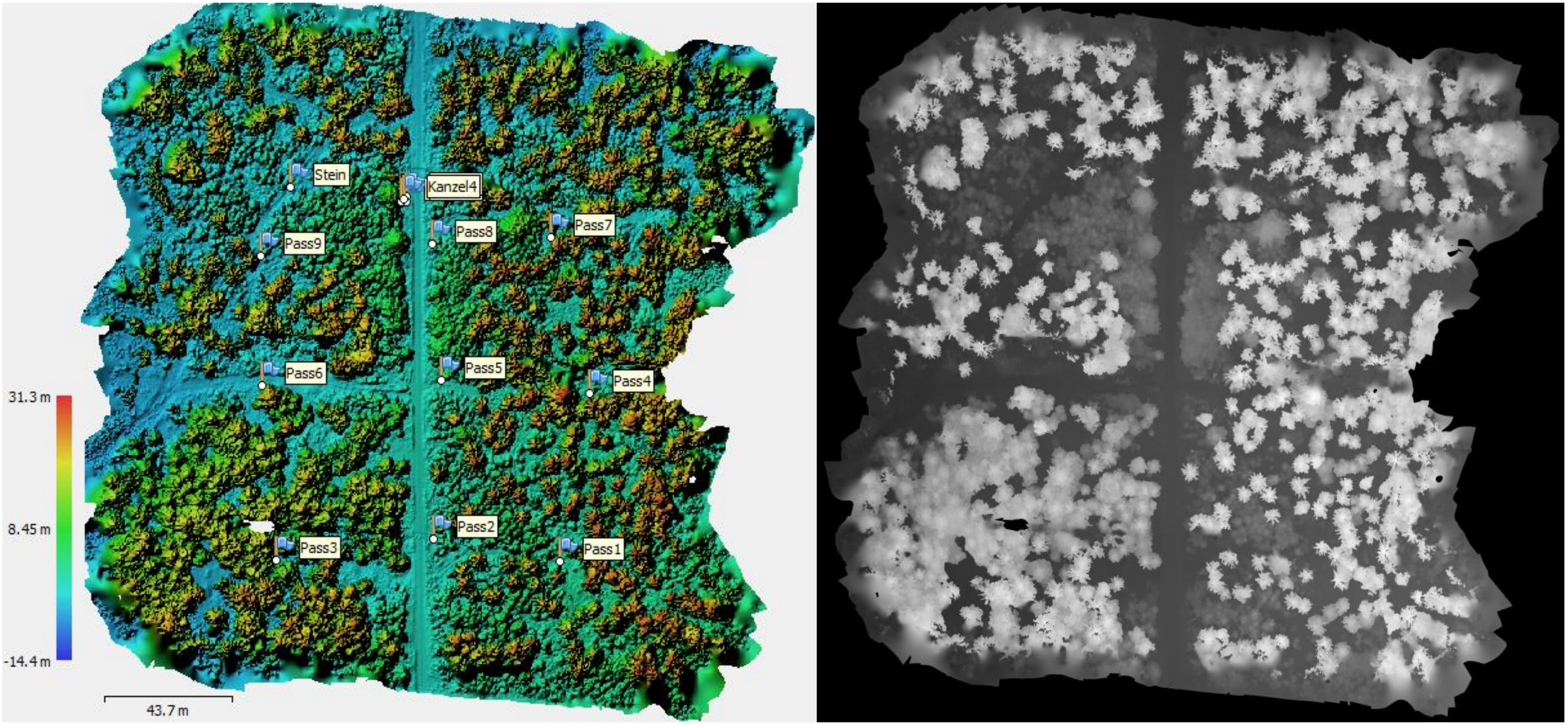

Fig. 16: Derived Digital Surface Model (DSM) in different displaying variants

6. Compute Orthomosaic

- Computation of orthomosaics based on DSM delivered best results
- Produced 6 separate AIRPHEN orthomosaics for different spectral bands
- Performed mutlilayer stack in raster package for RStudio

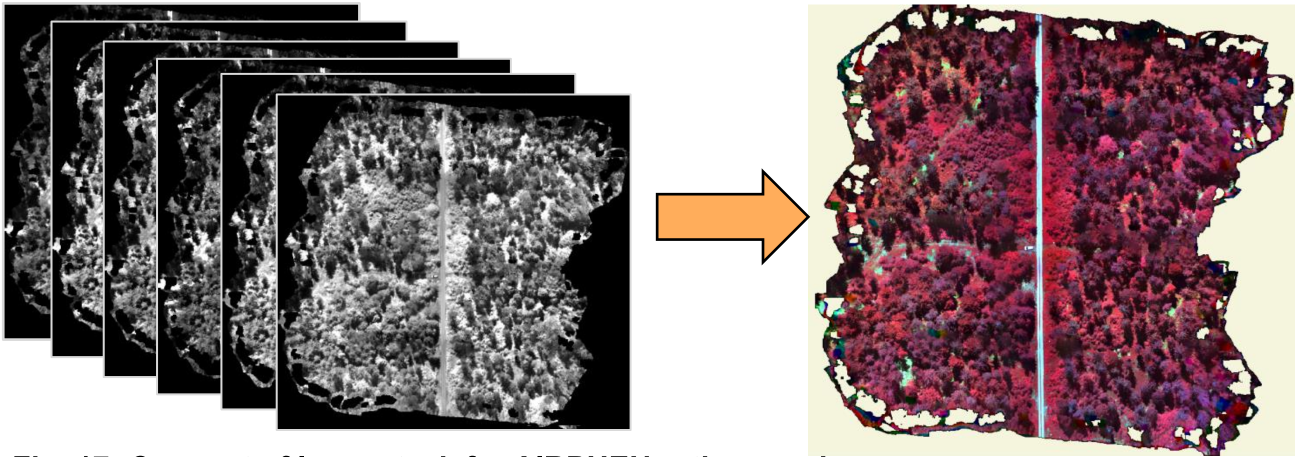

Fig. 17: Concept of layer stack for AIRPHEN orthomosaics

AIRPHEN Multilayer Stack

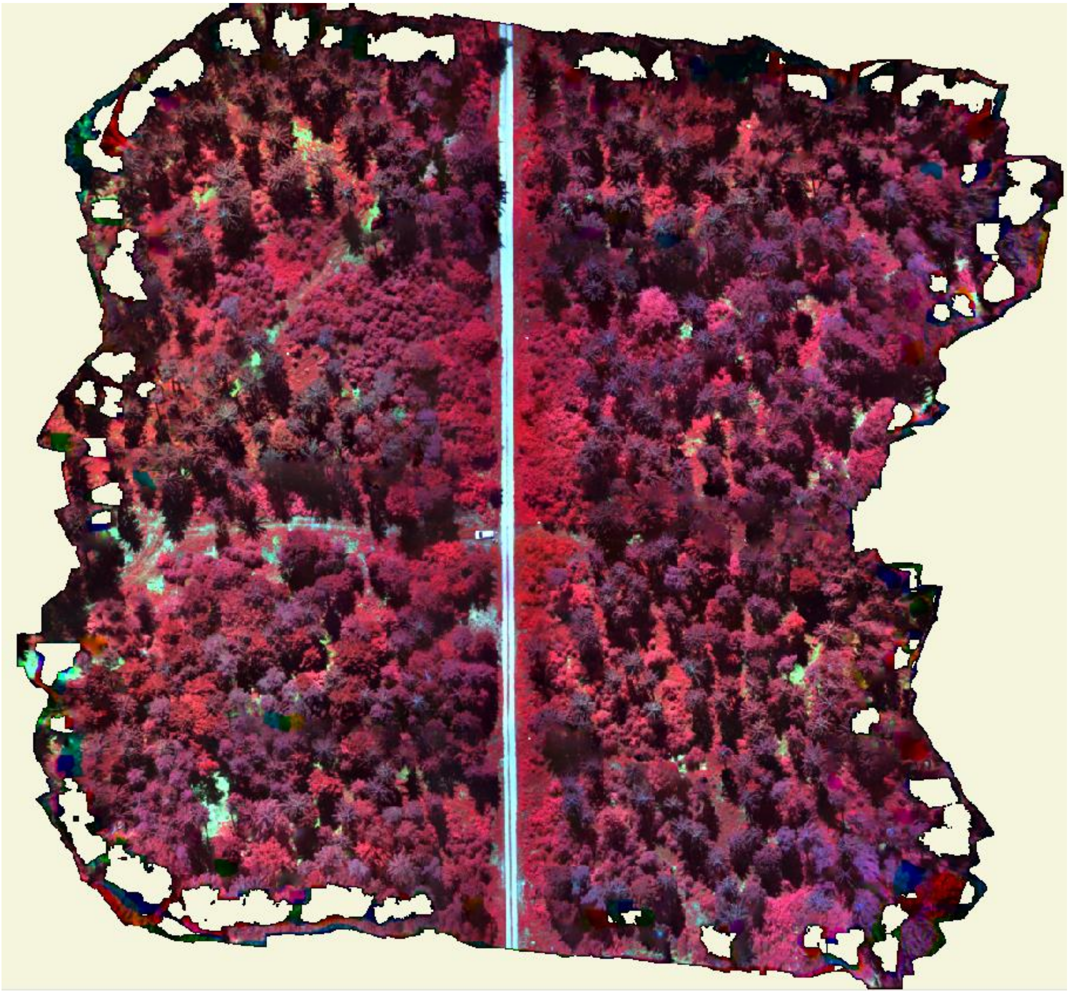

Fig. 18: Multilayer Stack in NIR (850 nm) / Red (675 nm) / Green (530 nm) composition

AIRPHEN Multilayer Stack

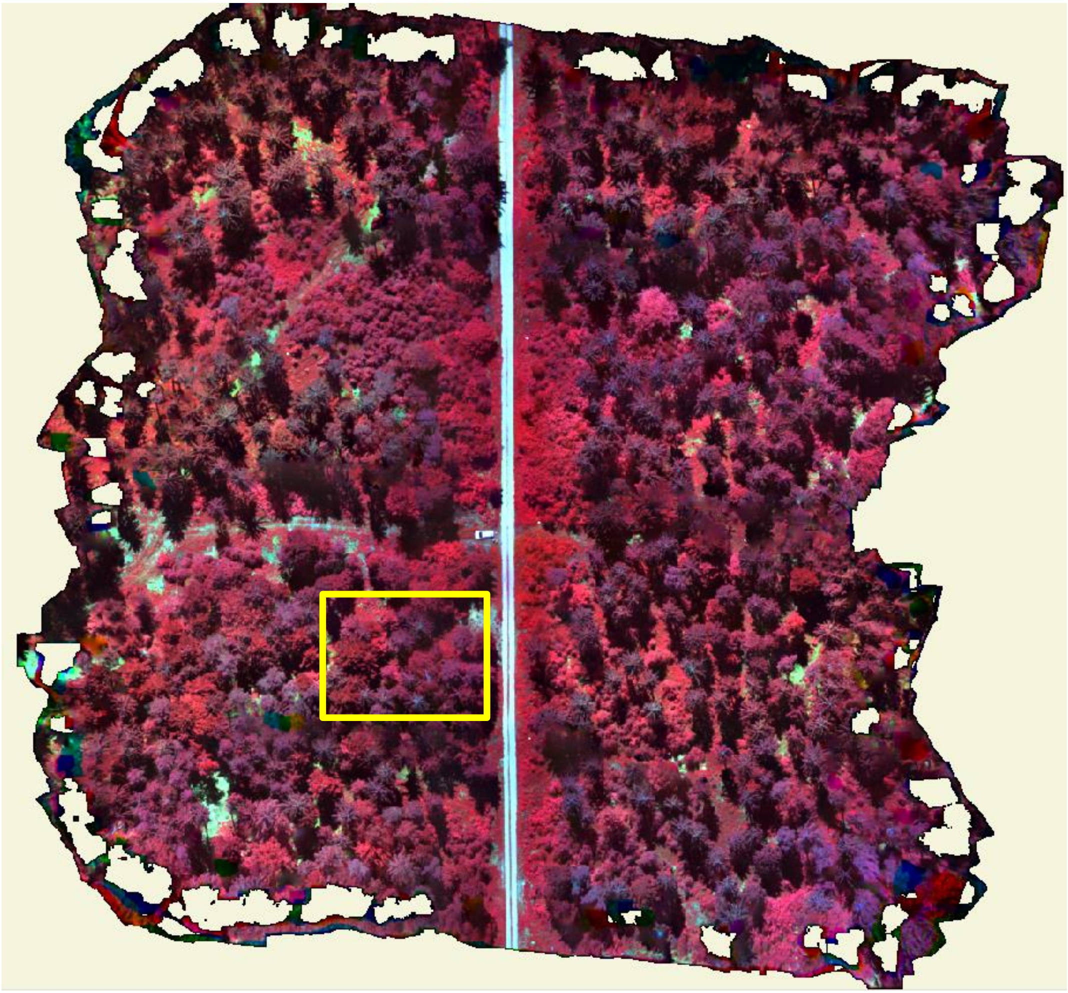

Fig. 18: Multilayer Stack in NIR (850 nm) / Red (675 nm) / Green (530 nm) composition

AIRPHEN Multilayer Stack

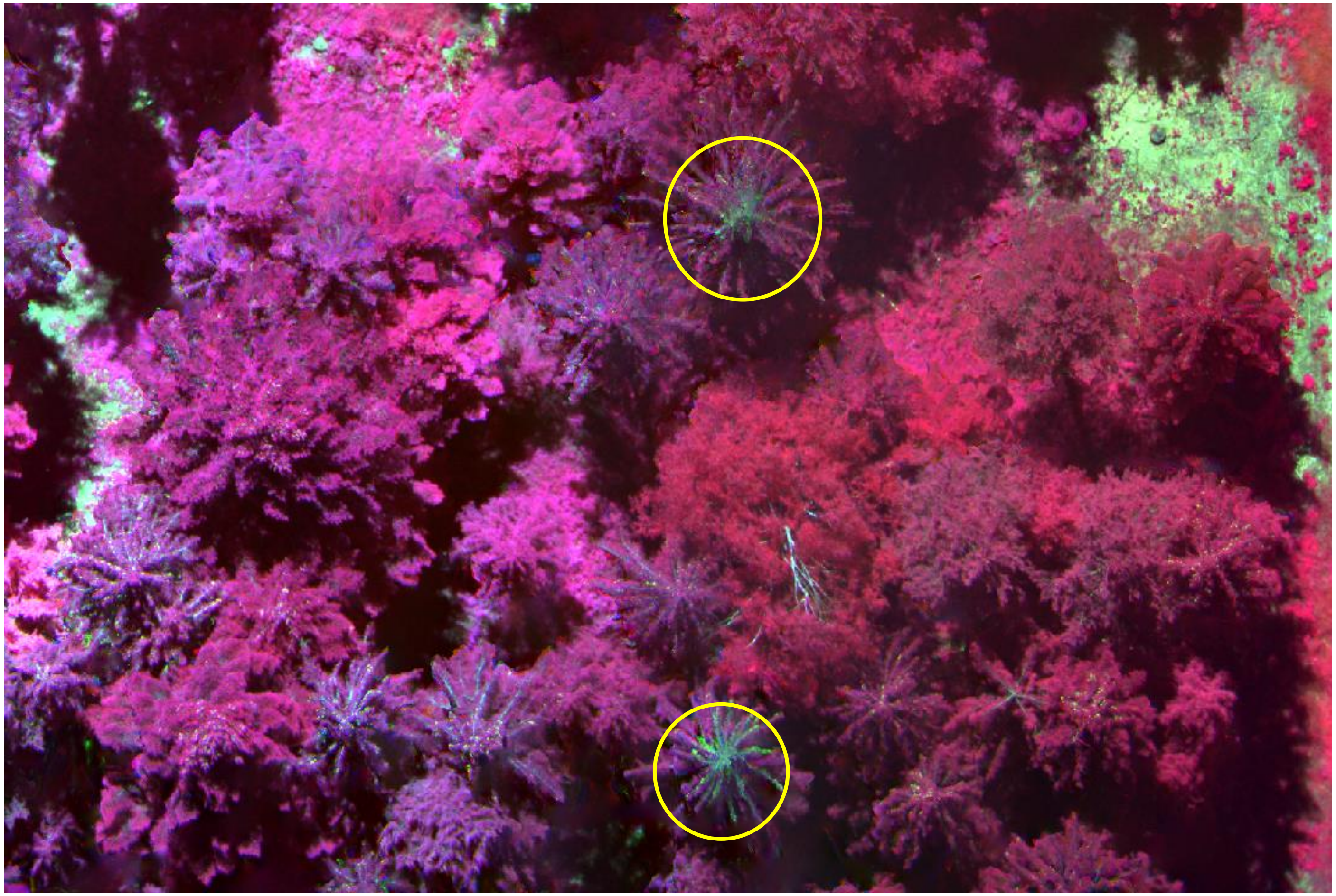

Fig. 19: Excerpt of Multilayer Stack with two stressed spruces (yellow marks)

Extraction of Pixel Values (DN)

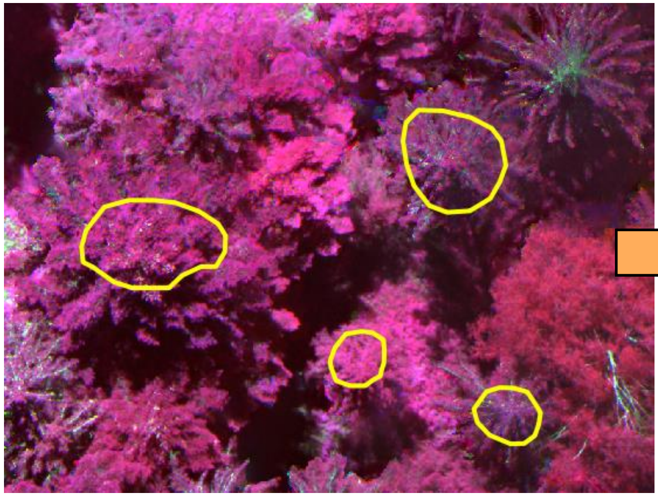

```r
#install.packages("raster")
library(raster)
library(matrixStats)
library(rgdal)

######################################### AIRPHEN ############################################################

setwd("D:/Max_Kampen/RStudio/Feasibility_Study")
images <- list.files(path="D:/Max_Kampen/11_Wald_Pengers", recursive = T, full.names=TRUE, pattern = "*stack_ortho.tif")
images
crowns <- shapefile("D:/Max_Kampen/ArcGIS/Tree_Crown_Analysis/Tree_Crown_Polygons.shp")
crowns@data
airphen <- brick(images[6])
airphen
DN_airphen <- extract(airphen, crowns)
matrix(unlist(DN_airphen), ncol = 6)
irphen_mean <- lapply(DN_airphen, colMeans)
N_airphen_means <- as.data.frame(do.call(rbind, airphen_mean))
names(DN_airphen_means) <- c(450, 530, 560, 675, 730, 850)
DN_airphen_20160928_means <- DN_airphen_means
wavelength <- as.numeric(names(DN_airphen_means))
plot(wavelength, DN_airphen_means[1,], type="n", ylim = c(0,2500), xlab="Wavelength [nm]", ylab="DN", main="Spectral Prof
lines(wavelength, DN_airphen_20160710_means[2,], col=1)
lines(wavelength, DN_airphen_20160730_means[2,], col=2)
lines(wavelength, DN_airphen_20160807_means[2,], col=3)
lines(wavelength, DN_airphen_20160924_means[2,], col=4)
lines(wavelength, DN_airphen_20160928_means[2,], col=5)
lines(wavelength, DN_airphen_means[6,], col=6)
lines(wavelength, DN_airphen_means[7,], col=7)
lines(wavelength, DN_airphen_means[8,], col=8)
lines(wavelength, DN_airphen_means[9,], col=9)

legend("to   ", c("20160710", "20160730", "20160807", "20160924", "20160928"), lty = c(1,1), col = c(1:5))
```

```
[[1]]
X20160928_beate_airphen_stack_ortho.1 X20160928_beate_airphen_stack_ortho.2 X20160928_beate_airphen_stack_ortho.3
                             242.9603                              854.1906                              938.3579
X20160928_beate_airphen_stack_ortho.4 X20160928_beate_airphen_stack_ortho.5 X20160928_beate_airphen_stack_ortho.6
                             377.2491                             1254.1007                             1035.9952

[[2]]
X20160928_beate_airphen_stack_ortho.1 X20160928_beate_airphen_stack_ortho.2 X20160928_beate_airphen_stack_ortho.3
                             429.9306                             1117.5688                             1116.5152
X20160928_beate_airphen_stack_ortho.4 X20160928_beate_airphen_stack_ortho.5 X20160928_beate_airphen_stack_ortho.6
                             822.8708                             1059.4570                              840.3369

[[3]]
X20160928_beate_airphen_stack_ortho.1 X20160928_beate_airphen_stack_ortho.2 X20160928_beate_airphen_stack_ortho.3
                             300.3461                              867.1381                              907.3860
X20160928_beate_airphen_stack_ortho.4 X20160928_beate_airphen_stack_ortho.5 X20160928_beate_airphen_stack_ortho.6
                             540.7473                             1260.7562                             1088.3786
```

Fig. 20: Concept of pixel value extraction using tree crown mask and raster package in RStudio

Initial Analysis – Tree Species

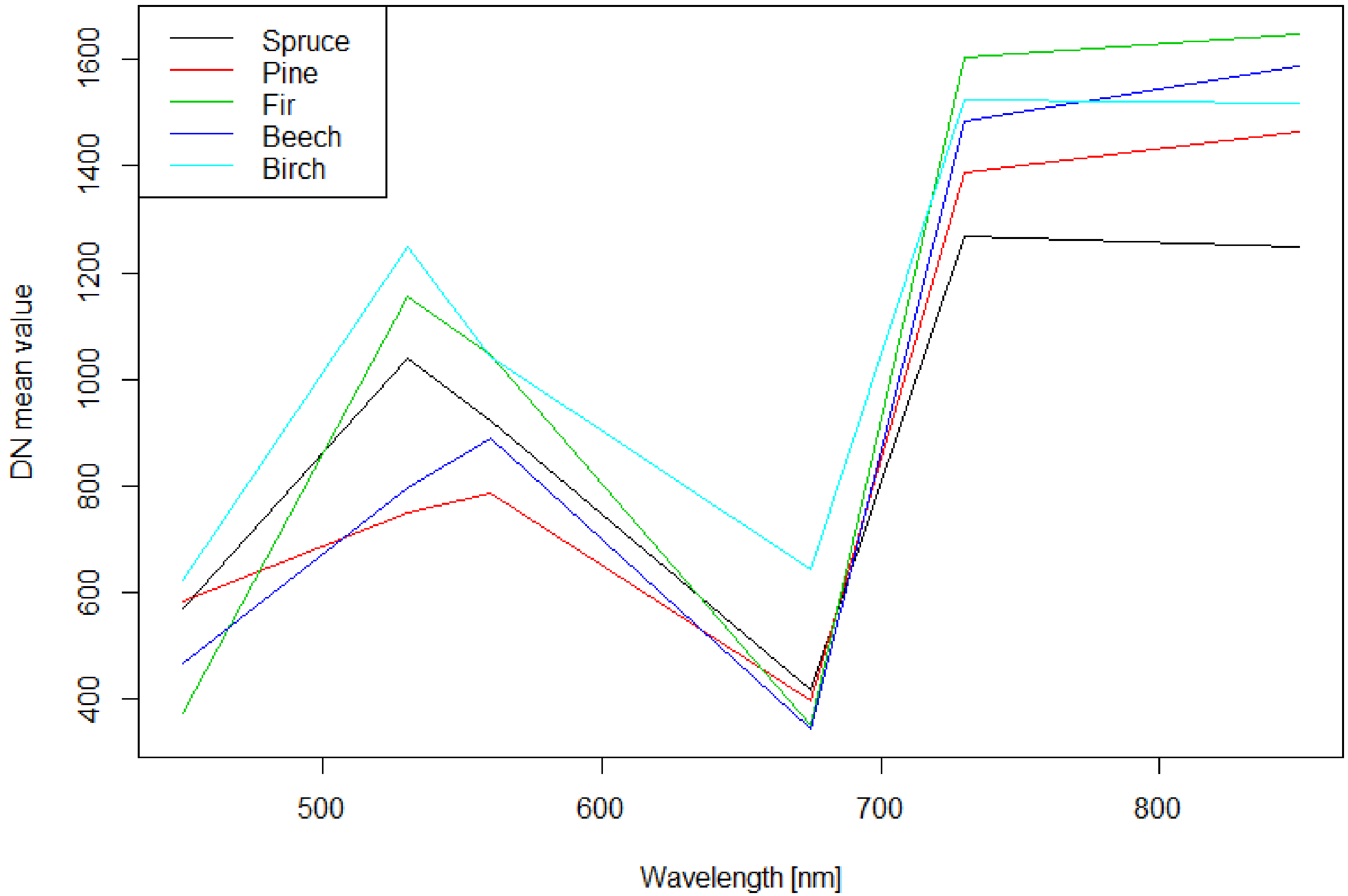

Fig. 21: Spectral profiles of occurring tree species, derived through plotting the mean digital number values (data from 10/07/2016) for each species against the respective wavelength of AIRPHEN spectral bands.

Initial Analysis – Health Status

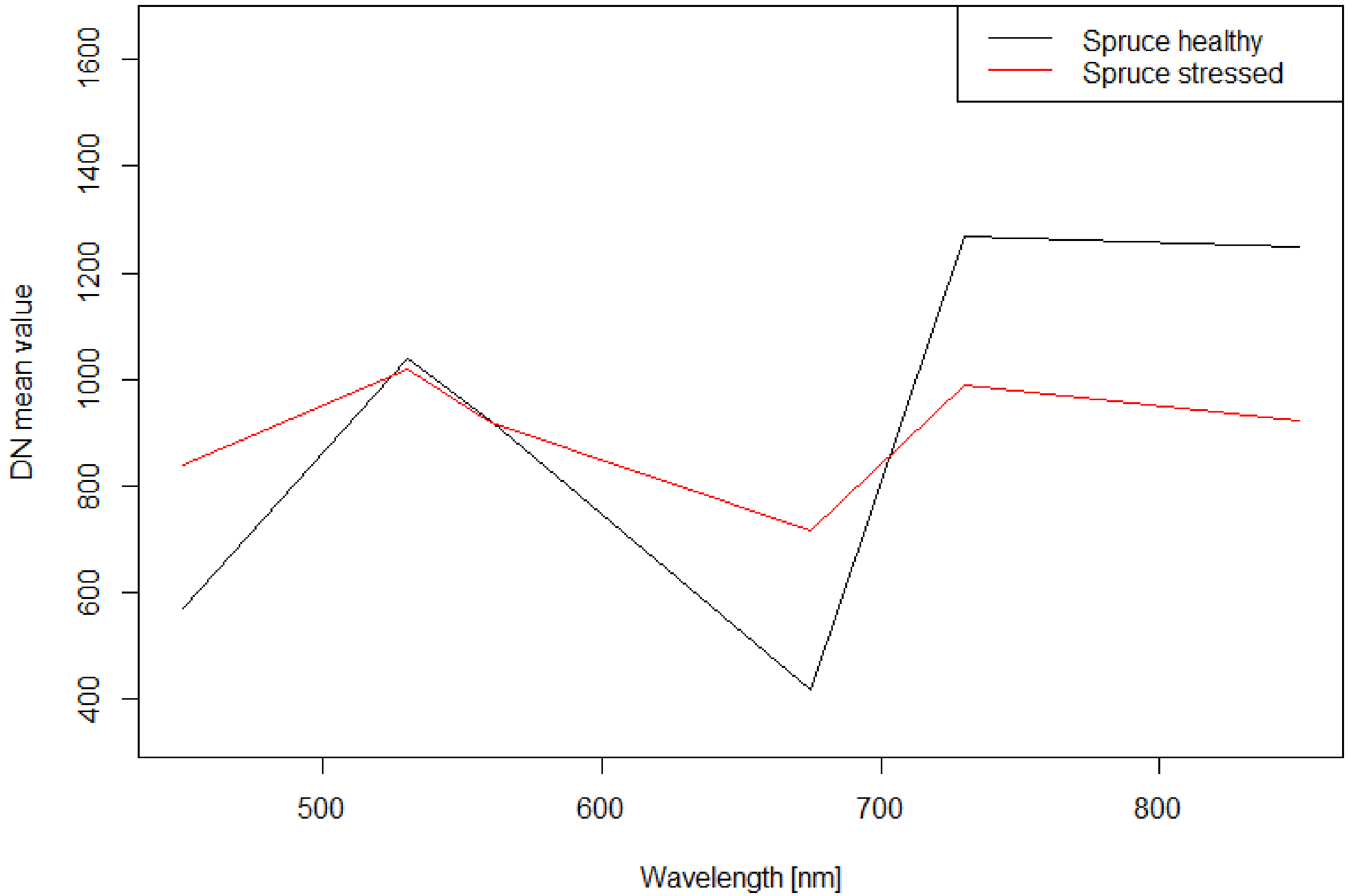

Fig. 22: Spectral profiles of a healthy and a stressed spruce, derived through plotting the mean digital number values (data from 10/07/2016) for both trees against the respective wavelength of AIRPHEN spectral bands.

Conclusion

- Results emphasize suitability of the data for future automatic tree species determination and classification
- Data is adequate for the detection of forest disturbances
- Early detection of bark beetle infestation is uncertain
- Gained valuable information for the improvement of future data acquisition

Outlook & Further Research tasks

- Improve data comparability by calculating reflectance values from DN
- Automatic Tree Segmentation via Canopy Height Models
- Exclusion of shaded crown parts via masking algorithms (Fassnacht et al., 2014)
- Implement normalization procedures and plant health indices (e.g. NDVI family)
- Optimization of flight planning

References

- Fassnacht, F. E., Latifi, H., Ghosh, A., Joshi, P. K., & Koch, B. (2014). Assessing the potential of hyperspectral imagery to map bark beetle-induced tree mortality. *Remote Sensing of Environment*, *140*, 533–548.
- Hijmans, R. J., & van Etten, J. (2014). raster: Geographic data analysis and modeling. *R Package Version*, *2*, 15.
- Immitzer, M., & Atzberger, C. (2014). Early Detection of Bark Beetle Infestation in Norway Spruce (Picea abies, L.) using WorldView-2 Data. *Photogrammetrie Fernerkundung Geoinformation*, (5), 351–367.
- Lausch, A., Heurich, M., Gordalla, D., Dobner, H.-J., Gwillym-Margianto, S., & Salbach, C. (2013). Forecasting potential bark beetle outbreaks based on spruce forest vitality using hyperspectral remote-sensing techniques at different scales. *Forest Ecology and Management*, *308*, 76–89.
- Lehmann, J., Nieberding, F., Prinz, T., & Knoth, C. (2015). Analysis of Unmanned Aerial System-Based CIR Images in Forestry—A New Perspective to Monitor Pest Infestation Levels. *Forests*, *6*(3), 594–612.
- Minařík, R., & Langhammer, J. (2016). Use of a Multispectral UAV Photogrammetry for Detection and tracking of Forest Disturbance Dynamics. *ISPRS - International Archives of the Photogrammetry, Remote Sensing and Spatial Information Sciences*, *XLI-B8*, 711–718.
- Näsi, R., Honkavaara, E., Lyytikäinen-Saarenmaa, P., Blomqvist, M., Litkey, P., Hakala, T. (2015). Using UAV-Based Photogrammetry and Hyperspectral Imaging for Mapping Bark Beetle Damage at Tree-Level. *Remote Sensing*, *7*(12), 15467–15493.
- Nevalainen, O., Honkavaara, E., Tuominen, S., Viljanen, N., Hakala, T., Yu, X. (2017). Individual Tree Detection and Classification with UAV-Based Photogrammetric Point Clouds and Hyperspectral Imaging. Remote Sensing, 9(3), 185.
- Torresan, C., Berton, A., Carotenuto, F., Di Gennaro, S. F., Gioli, B., Matese, A. (2017). Forestry applications of UAVs in Europe: a review. International Journal of Remote Sensing, 38(8-10), 2427-2447.

Image Sources

- Slide 9:
  - Fig. 3: Tetracam ADC Snap
    http://www.termocam.it/images/stories/virtuemart/product/adc-snap.jpg
    [16.01.2017]
  - Fig. 4: AIRPHEN
    http://www.hiphen-plant.com/docs/airphen_solid_coupe.png [16.01.2017]

Thanks for your attention!

Universität für Bodenkultur Wien
Department für Raum, Landschaft und Infrastruktur

Student

Max Kampen BSc.

Am Platz 4 / 6

1130 Vienna, AUSTRIA

Email: max.kampen@hnee.de

max.kampen@students.boku.ac.at

Tel: +43 (0)677 623 631 89

+49 (0)151 207 265 83

Supervisor

Dipl.-Ing. Markus Immitzer MSc.

Peter-Jordan-Straße 82

1190 Vienna, AUSTRIA

Email: markus.immitzer@boku.ac.at

Tel: +43 1 47654-85732